ELSEVIER

Thermochimica Acta 299 (1997) 87–93

thermochimica
acta

Preparation, crystal structure, thermal decomposition mechanism and thermodynamical properties of $[Dy(NTO)_2(H_2O)_6]\cdot NTO\cdot 4H_2O$

Hu Rongzu[a,*], Song Jirong[b], Li Fuping[a], Kang Bing[a], Kuong Yanghui[a], Mao Zhihua[c],
Zhou Zonghua[c], Hong Zhou[c]

[a] *Xian Modern Chemistry Research Institute, Xian 710065, Shaanxi, P.R. China*
[b] *Department of Chemical Engineering, Northwest University, Xian 710069, P.R. China*
[c] *Department of Chemistry and Testing and Analytical Center, Sichuan University, Chengdu 610064, P.R. China*

Abstract

$[Dy(NTO)_2(H_2O)_6]\cdot NTO\cdot 4H_2O$ was prepared by mixing the aqueous solution of lithium 3-nitro-1,2,4-triazol-5-onate and the dilute nitric acid solution of dysprosium oxide. The single crystal structure has been determined by a four-circle x-ray diffractometer. The crystal is monoclinic, space group $P2_1/n$ with crystal parameters of $a = 1.0094(1)$ nm, $b = 1.2586(2)$ nm, $c = 1.8845(2)$ nm, $\beta = 106.31(1)^0$, $V = 2.2978\ \mathrm{nm}^3$, $Z = 4$, $\mu = 33.890\ \mathrm{cm}^{-1}$, $F(000) = 1444$, $D_x = 2.11\ \mathrm{g\,cm}^{-3}$, $\lambda(\mathrm{Mo}K_\alpha) = 0.071073$ nm. The final R is 0.041. Based on the thermal analysis, the thermal decomposition mechanism of $[Dy(NTO)_2(H_2O)_6]\cdot NTO\cdot 4H_2O$ has been derived. From measurements of the enthalpy of solution in water of $[Dy(NTO)_2(H_2O)_6]\cdot NTO\cdot 4H_2O$ at 298.15 K, the standard enthalpy of formation, lattice energy, lattice enthalpy and standard enthalpy of dehydration have been determined as $-(3894.5 \pm 6.5)$, -4525, -4560 and 306.9 $\mathrm{kJ\,mol}^{-1}$, respectively.

Keywords: Crystal structure; Dysprosium coordination; Enthalpy of solution; Lattice energy; Lattice enthalpy; NTO salt; Preparation; Standard enthalpy of dehydration; Standard enthalpy of formation; Thermal decomposition mechanism

1. Introduction

Much attention has been paid to 3-nitro-1,2,4-triazol-5-one (NTO) as a high energy and low sensitivity energetic material. Its metal salts also have some potential uses in ammunition, especially its rare earth metal salts as catalyst. Therefore the authors prepared the single crystal of $[Dy(NTO)_2(H_2O)_6]\cdot NTO\cdot 4H_2O$, measured its structure and studied its thermal decomposition mechanism and thermodynamic properties.

2. Experimental

2.1. Materials

$[Dy(NTO)_2(H_2O)_6]\cdot NTO\cdot 4H_2O$ used in this research work was prepared according to the following method: An appropriate amount of NTO was put into the distilled water, then stirred and titrated with an aqueous solution of lithium hydroxide under 60°C until pH reached 6~7. The resulted solution was gradually dropped into a dilute nitric acid solution of dysprosium oxide at 60°C, then stirred and heated at 60°C for 30 min. This solution was allowed to stand for 12 h until a yellow precipitate was formed. The precipitate was recrystallized with distilled water at the culture box at 25°C to obtain the yellow single

---

*Corresponding author.

PII S0040-6031(97)00140-8

crystal for X-ray measurement. Its purity was more than 99.6%. Dimensions of the single crystal were $0.23 \times 0.25 \times 0.30\ \mathrm{mm}^3$. The conductivity of deionized water used in the experiment was $5.48 \times 10^{-8}\ \mathrm{s\ cm}^{-1}$.

2.2. *Experimental equipment and conditions*

In the determination of the structure of the single crystal, X-ray intensities were recorded by a CAD4PDP11/44 automatic diffractometer with graphite-monochromatized MoK_α radiation, $\lambda = 0.71073$ Å. The 3284 independent reflections were obtained in the range of $2° \leq \theta \leq 25°$, among which 2506 with $I > 3.0\sigma(I)$ were used for the determination and refinement of crystal structure. The coordinates of Dy atom were obtained by the Patterson method and those of the other atoms by difference Fourier synthesis. Refinement was performed by block-diagonal least-square methods using anisotropic thermal parameters for non-hydrogen atoms and fixed thermal parameters for hydrogen atoms.

The thermal decomposition process was studied using a TG technique on a Delta Series TGA 7 (Perkin Elmer Co., USA). The conditions of TG were as follows: sample mass about 1 mg, heating rate $10°\mathrm{C\ min}^{-1}$; atmosphere flowing N_2/O_2 mixture (with a ratio in air). The DSC experiments were carried out with a model CDR-1 differential scanning calorimeter with a sample pan of aluminium (diameter 5 mm×3 mm), whose side was rolled up. The conditions of DSC were as follows: sample mass about 1 mg; heating rate $10°\mathrm{C\ min}^{-1}$; atmosphere static air; reference sample α-Al_2O_3; thermocouple plate Ni/Cr-Ni/Si. The infrared spectra of the decomposition residues were recorded in KBr discs on a 60 SXR FT-IR spectrometer (Nicolet Co., USA) at $4\ \mathrm{cm}^{-1}$ resolution.

All measurements of the enthalpy of solution in deionized water were made using a Calvet microcalorimeter, type BT215 from Setaram, France and operated at 298.15 ± 0.005 K.

The experimental precision and accuracy of enthalpies of solution were frequently checked by measurement of the enthalpies of solution ($\Delta_{\mathrm{sol}}H^0_\infty$) of crystalline KCl in deionized water at 298.15 K. The experimental value of $\Delta_{\mathrm{sol}}H^0_\infty = (17.217 \pm 0.053)\ \mathrm{kJ\ mol}^{-1}$ is in excellent agreement with that of $\Delta_{\mathrm{sol}}H^0_\infty = 17.234\ \mathrm{kJ\ mol}^{-1}$ reported in the literature [1].

3. Results and discussion

3.1. *Crystal structure*

The crystal structure was found to be monoclinic, which belongs to space group $P2_1/n$ with crystallographic parameters of $a = 1.0094(1)$ nm, $b = 1.2586(2)$ nm, $c = 1.8845(2)$ nm, $\beta = 106.31\ (1)°$, V=2.2978(7) nm^3, Z=4, μ=33.890 cm^{-1}, $F(000) = 1444$, $Dx = 2.11\ \mathrm{g\ cm}^{-3}$. The final $R = 0.041$, $Rw = 0.047$ (unit weight), and $(\Delta/\sigma)_{\max} = 0.68$.

The atom coordinates, thermal parameters, bond lengths and bond angles are summarized in Tables 1–3. The molecular structure and atom labeling are shown in Fig. 1 and the packing of the molecule in the crystal lattice is illustrated in Fig. 2.

The analytical results indicate that the Dy atom, the two carbonyl oxygen of the two NTO cycles and six water molecules form the hydrated cation $[Dy(NTO)_2(H_2O)_6]^+$ which was a distorted dodecahedron. By combining it with the NTO anion, $[Dy(NTO)_2(H_2O)_6]\cdot NTO$ was obtained. There are four water molecules of crystallization in the crystal, denoted as $[Dy(NTO)_2(H_2O)_6]\cdot NTO\cdot 4H_2O$. In addition, there are hydrogen bonds among six coordination water molecules, four water molecules of crystallization and three NTO, shown in Fig. 1 and Table 2.

As shown in Table 2, the distance between Dy and the coordination water is 0.2367–0.2414 nm, between Dy and the carbonyl oxygen of NTO cycle is 0.233–0.234 nm. Because of the induction effect of Dy^{3+}, the conjugate π-electrons of carbonyl oxygen O11 and O21 are partly shared between Dy-O11 and Dy-O21 and the coordination bonds become shorter.

In three NTO cycles, the bond distances are all 0.130–0.137, except Ci2-Ni2 ($i = 1, 2, 3$) (0.130–0.1308 nm), as compared with other bond distances (0.1339-0.137 nm), which are obviously shorter. The bond length of Cil-Oil ($i = 1, 2$) (0.127 nm) is only slightly greater than that of C31-O31 (0.125 nm) because of the induction effect of Dy^{3+}.

According to the calculation, the atoms in the three NTO cycles are all coplanar. The equations of the

Table 1
Positional parameters and Beq (in nm^2)

Atom	x	y	z	Beq
Dy	0.24245(5)	0.00235(4)	0.7486(3)	0.0118(1)
Ow1	0.377(2)	−0.0591(7)	0.8651(6)	0.017(3)
Ow2	0.1083(6)	−0.055(2)	0.6298(7)	0.016(4)
Ow3	0.3713(7)	−0.1374(5)	0.710(2)	0.016(2)
Ow4	0.474(1)	0.0586(7)	0.7594(6)	0.023(3)
Ow5	0.1437(3)	−0.160(1)	0.7720(8)	0.016(4)
Ow6	0.0075(5)	0.0383(3)	0.742(1)	0.022(6)
Ow7	0.2494(8)	0.0326(3)	0.3578(3)	0.030(3)
Ow8	0.7819(5)	0.448(1)	0.6716(7)	0.046(5)
Ow9	0.3598(9)	0.3436(6)	0.311(1)	0.061(7)
Ow10	0.619(1)	0.267(1)	0.7222(6)	0.065(3)
O11	0.242(2)	0.144(1)	0.829(1)	0.013(7)
O12	0.390(1)	0.286(2)	1.1239(7)	0.026(3)
O13	0.4160(7)	0.3984(5)	1.041(2)	0.020(2)
O21	0.238(1)	0.1478(8)	0.6713(7)	0.012(3)
O22	0.0783(3)	0.399(1)	0.4547(8)	0.020(4)
O23	0.1129(5)	0.2872(2)	0.376(1)	0.028(6)
O31	0.5770(9)	0.0715(5)	0.4156(3)	0.018(3)
O32	0.4489(4)	0.401(1)	0.5865(7)	0.032(5)
O33	0.3858(6)	0.4253(4)	0.4690(9)	0.029(4)
N11	0.2482(9)	0.0973(7)	0.9492(5)	0.014(2)
N12	0.288(2)	0.1416(8)	1.0180(6)	0.015(3)
N13	0.3276(7)	0.254(2)	0.9315(9)	0.009(4)
N14	0.3839(9)	0.3115(6)	1.060(2)	0.014(2)
N21	0.249(1)	0.1006(8)	0.5538(7)	0.014(4)
N22	0.2148(3)	0.145(1)	0.4848(8)	0.014(4)
N23	0.1635(6)	0.2576(3)	0.567(1)	0.010(6)
N24	0.115(1)	0.3119(6)	0.4387(3)	0.014(3)
N31	0.5862(5)	0.124(1)	0.5357(6)	0.015(4)
N32	0.5487(6)	0.2095(5)	0.5699(9)	0.016(5)
N33	0.4947(8)	0.2349(7)	0.4452(5)	0.013(2)
N34	0.441(2)	0.3731(8)	0.5241(7)	0.017(3)
C11	0.2712(7)	0.164(2)	0.8976(9)	0.009(4)
C12	0.3323(9)	0.2332(7)	1.002(2)	0.008(2)
C21	0.218(1)	0.1672(8)	0.6029(7)	0.010(4)
C22	0.1654(3)	0.235(1)	0.4980(9)	0.009(5)
C31	0.5537(6)	0.1381(3)	0.460(1)	0.014(6)
C32	0.497(1)	0.2705(7)	0.5125(4)	0.014(4)
H11	0.2118(6)	0.035(1)	0.9382(6)	0.04
H21	0.2902(3)	0.035(1)	0.5739(9)	0.04
H31	0.6391(8)	0.076(2)	0.565(1)	0.04
Hw11	0.4433	−0.0292	0.8828	0.04
Hw12	0.3613	−0.1093	0.8847	0.04
Hw21	0.0292	−0.0292	0.6015	0.04
Hw22	0.1113	−0.1113	0.6171	0.04
Hw31	0.3906	−0.1093	0.6679	0.04
Hw32	0.3339	−0.1933	0.7011	0.04
Hw41	0.4707	0.1386	0.7656	0.04
Hw42	0.5297	0.0292	0.7851	0.04
Hw61	0.0546	0.0292	0.7324	0.04
Hw62	0.0000	0.0839	0.7656	0.04
Hw71	0.2500	0.0839	0.3828	0.04
Hw72	0.3320	0.0546	0.3496	0.04
Hw81	0.8320	0.3906	0.6992	0.04
Hw82	0.8066	0.4707	0.6679	0.04
Hw92	0.4160	0.3320	0.3496	0.04
Hw101	0.5820	0.2207	0.7148	0.04
Hw102	0.6933	0.2500	0.7500	0.04
Hw91	0.3733(8)	0.2865(6)	0.297(1)	0.04
Hw51	0.1953	−0.2226	0.7851	0.04
Hw52	0.0566	−0.1679	0.7675	0.04

Table 2
Bond distances (in nm)

Dy-Ow1	0.2367(10)	Dy-O21	0.2330(12)
Dy-Ow2	0.2380(12)	O11-C11	0.127(3)
Dy-Ow3	0.2414(14)	O12-N14	0.123(3)
Dy-Ow4	0.2393(10)	O13-N14	0.122(2)
Dy-Ow5	0.2369(13)	O21-C21	0.127(2)
Dy-Ow6	0.2382(6)	O22-N24	0.1223(15)
Dy-O11	0.234(2)	O23-N24	0.123(2)
O32-N34	0.121(2)	O31-C31	0.125(2)
O33-N34	0.122(2)	N22-C22	0.130(2)
N11-N12	0.1365(14)	N23-C21	0.1357(14)
N11-C11	0.135(2)	N23-C22	0.134(3)
Ow6-Ow9	0.269(1)	N24-C22	0.146(2)
Ow1-O22	0.302(1)	N31-N32	0.136(2)
Ow7-O31	0.3216(11)	N31-N31	0.138(3)
O31-N21	0.2746(13)	N32-C32	0.1308(15)
Ow2-O13	0.294(2)	N33-C31	0.1350(10)
Ow8-Ow4	0.282(1)	N33-C32	0.1339(12)
Ow2-N13	0.281(3)	N34-C32	0.1453(15)
Ow3-O11	0.299(2)	Ow6-Ow2	0.284(1)
Ow3-O31	0.270(3)	Ow1-N23	0.272(1)
Ow4-Ow10	0.318(2)	Ow7-N22	0.288(2)
Ow5-O21	0.278(2)	Ow7-N31	0.297(2)
N12-C12	0.130(2)	Ow8-O12	0.334(2)
N13-C11	0.135(2)	O32-N11	0.3127(14)
N13-C12	0.134(3)	Ow9-Ow10	0.2888(15)
N14-C12	0.146(3)	Ow9-N33	0.286(2)
N21-N22	0.137(2)	Ow4-Ow8	0.2816(12)
N21-C21	0.135(2)	Ow5-Ow10	0.2843(14)

planes are as follows:

$$-0.9100x + 0.3871y - 0.1482z - 0.2229 = 0 \qquad \text{(I)}$$

$$-0.8954x - 0.4020y - 0.1913z + 2.0508 = 0 \qquad \text{(II)}$$

$$-0.9079x - 0.4064y - 0.1027z + 4.4249 = 0 \qquad \text{(III)}$$

Table 3
Bond angles(°)

Ow1-Dy-Ow2	143.1(5)	Ow1-Dy-Ow3	79.7(7)
Ow1-Dy-Ow4	74.0(4)	Ow6-Dy-O11	73.0(5)
Ow1-Dy-Ow5	72.9(4)	Ow6-Dy-O21	88.3(4)
Ow1-Dy-Ow6	114.6(6)	O11-Dy-O21	78.5(6)
Ow1-Dy-O11	75.7(5)	N12-N11-C11	112.0(1)
Ow1-Dy-O21	138.0(4)	N11-N12-C12	100.0(2)
Ow2-Dy-Ow3	73.1(6)	C11-N13-C12	101.0(1)
Ow2-Dy-Ow4	117.1(4)	O12-N14-O13	125.0(2)
Ow2-Dy-Ow5	75.8(5)	O12-N14-C12	118.0(2)
Ow2-Dy-Ow6	73.3(5)	O13-N14-C12	117.0(3)
Ow2-Dy-O11	137.5(5)	N22-N21-C21	111.0(1)
Ow2-Dy-O21	75.3(5)	N21-N22-C22	101.0(1)
Ow3-Dy-Ow4	69.3(3)	C21-N23-C22	101.0(1)
Ow3-Dy-Ow5	73.6(4)	O22-N24-O23	125.4(9)
Ow3-Dy-Ow6	137.2(3)	O22-N24-C22	118.0(1)
Ow3-Dy-O11	147.9(5)	O23-N24-C22	116.6(9)
Ow3-Dy-O21	107.8(7)	N32-N31-C31	112.0(1)
Ow4-Dy-Ow5	133.7(3)	N31-N32-C32	100.0(1)
Ow4-Dy-Ow6	151.8(2)	C31-N33-C32	103.0(1)
Ow4-Dy-O11	84.1(5)	O32-N34-O33	124.0(1)
Ow4-Dy-O21	70.8(4)	O32-N34-C32	119.0(1)
Ow5-Dy-Ow6	73.1(2)	O33-N34-C32	117.0(1)
Ow5-Dy-O11	117.3(6)	O11-C11-N11	125.0(2)
Ow5-Dy-O21	149.1(4)	O11-C11-N13	126.0(2)
N11-C11-N13	108.0(1)	N22-C22-N24	120.0(1)
N12-C12-N13	119.0(2)	N23-C22-N24	121.0(1)
N12-C12-N14	120.0(2)	O31-C31-N31	124.8(8)
N13-C12-N14	121.0(2)	O31-C31-N33	128.0(2)
O21-C21-N21	125.0(1)	N31-C31-N33	107.0(1)
O21-C21-N23	126.0(1)	N32-C32-N33	118.9(9)
N21-C21-N23	109.0(1)	N32-C32-N34	118.6(9)
N22-C22-N23	119.0(1)	N33-C32-N34	122.4(8)

The dihedral angles between planes (I) and (II),(I) and (III), (II) and (III) are 46.6°, 46.8° and 5.1°, respectively, so planes (II) and (III) are almost parallel, and the angles of inclination between plane (III) and (II) are equal. Moreover the distances from O12 and O13, O22 and O23, O32 and O33 to the relevant planes of 1,2,4-triazole cycle are −0.0010 nm and +0.0123 nm, −0.0094 nm and +0.0081 nm, −0.0009 nm and +0.0097 nm, respectively. These show that two oxygen atoms in 3-nitro lie over and under the relevant planes of 1,2,4-triazole cycle, but out on the planes.

3.2. Mechanism of thermal decomposition of $[DY(NTO)_2(H_2O)_6]\cdot NTO\cdot 4H_2O$

The TG-DTG curves for $[Dy(NTO)_2(H_2O)_6]\cdot NTO\cdot 4H_2O$ are shown in Fig. 3. The DSC curve of

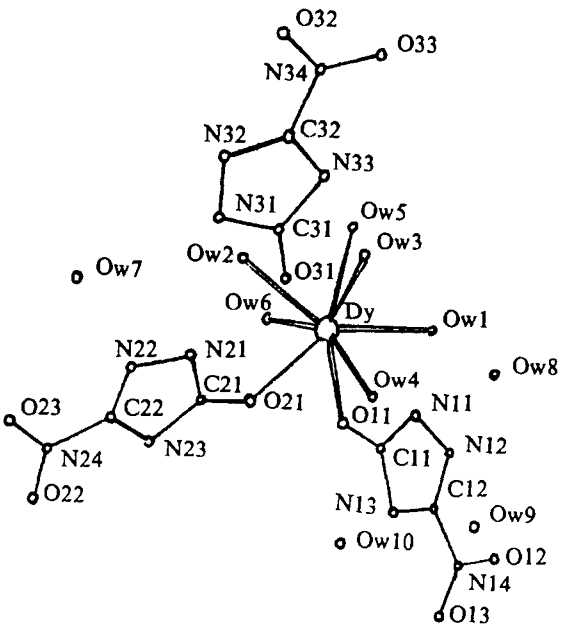

Fig. 1. Molecular structure of $[Dy(NTO)_2(H_2O)_6]\cdot NTO\cdot 4H_2O$.

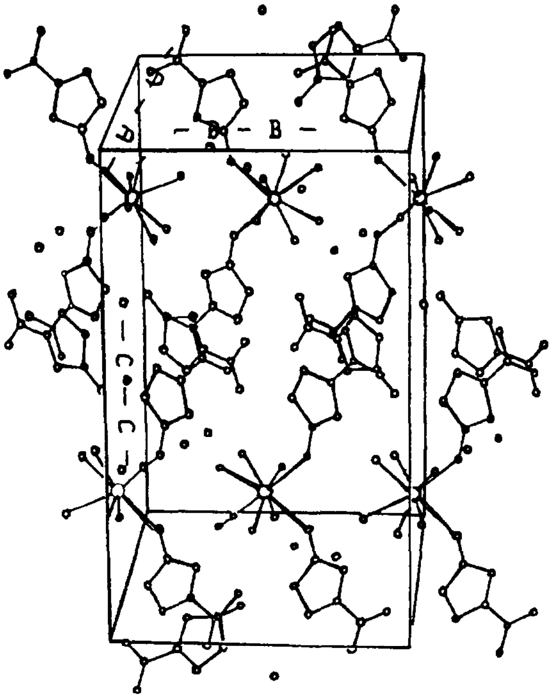

Fig. 2. Packing of the molecule $[Dy(NTO)_2(H_2O)_6].NTO.4H_2O$ in the crystal lattice.

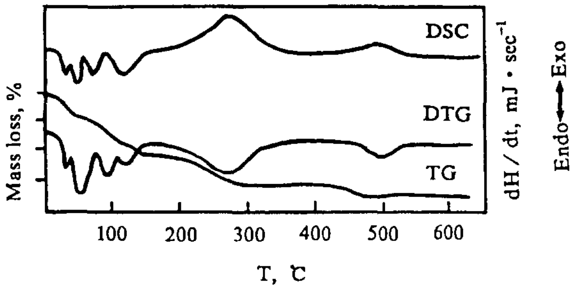

Fig. 3. DSC and TG-DTG curves for $[Dy(NTO)_2(H_2O)_6]\cdot NTO\cdot 4H_2O$ at a heating rate of 10°C min^{-1}.

Table 4
Mass losses and corresponding temperatures for $[Dy(NTO)_2(H_2O)_6].NTO.4H_2O$

T(°C)	Mass loss (%)		No. of lost H_2O
	Exp.	Theory	
40–68	4.9	4.9	2
68–92	9.5	9.9	2
92–112	15.5	14.8	2
112–183	22.0	24.7	4
183–380	53.0	—	
380–600	74.0	74.4	

Fig. 3 shows that there are four endothermic and two exothermic processes at temperatures higher than 40°C. In Table 4, the initial and final temperatures of the thermal decomposition processes and the mass losses observed between these temperatures in the TG curve are given. It can be seen from Fig. 3 and Table 4 that the endothermic processes result in a loss of ten water molecules. Further decomposition of the dehydrated salt $Dy(NTO)_3$ would occur on heating. The decomposition products are the same as that of $[Dy(NTO)_3]$ in Ref. [2]. The characteristic absorption peaks of $Dy(OCN)_3$, $Dy_2(CO_3)_3$ and polymers containing the -CO-NH-group formed after the first exothermic peak appear at 2189 and 1185, 1503 and 836, and 3382, 1634, 1556 and 1378 cm^{-1}, respectively. These observations show that the decomposition residue for this stage is a mixture. The amount of each component can not be determined from the present experiments and it is impossible to determine the decomposition change stoichiometrically. The characteristic absorption peaks of the residue formed after the second exothermic peak at 556 and 407 cm^{-1} are assigned to Dy_2O_3. At the end of this stage, the residue amounted to 26.0%. This value is in good agreement with the calculated loss of 25.6%.

On the bases of experimental and calculated results, the thermal decomposition mechanism of $[Dy(NTO)_2(H_2O)_6]\cdot NTO\cdot 4H_2O$ is postulated to be as follows:

$$\mathrm{Dy(NTO)_3\cdot 10H_2O} \xrightarrow[40-68^\circ\mathrm{C}]{-2\mathrm{H_2O}}$$

$$\mathrm{Dy(NTO)_3\cdot 8H_2O} \xrightarrow[68-92^\circ\mathrm{C}]{-2\mathrm{H_2O}}$$

$$\mathrm{Dy(NTO)_3\cdot 6H_2O} \xrightarrow[92-112^\circ\mathrm{C}]{-2\mathrm{H_2O}}$$

$$\mathrm{Dy(NTO)_3\cdot 4H_2O} \xrightarrow[112-183^\circ\mathrm{C}]{-4\mathrm{H_2O}}$$

$$\mathrm{Dy(NTO)_3} \xrightarrow[183-380^\circ\mathrm{C}]{} \mathrm{Dy(OCN)_3 + Dy_2(CO_3)_3}$$

$$+\,\mathrm{polymers} \xrightarrow[380-600^\circ\mathrm{C}]{} \mathrm{Dy_2O_3}.$$

3.3. Enthalpy of solution in water of $[Dy(NTO)_2(H_2O)_6]\cdot NTO\cdot 4H_2O$

Results for the enthalpy of solution of $(Dy(NTO)_2(H_2O)_6]\cdot NTO\cdot 4H_2O$ in deionized water at 298.15 K are reported in Table 5, where $\Delta_{sol}H^{\theta}_{m}$ denotes the enthalpy of solution in water of $[Dy(NTO)_2(H_2O)_6]\cdot NTO\cdot 4H_2O$, m is the mass of

Table 5
Enthalpy of solution in water of $[Dy(NTO)_2(H_2O)_6]\cdot NTO\cdot 4H_2O$ (cr) at 298.15 K

m(mg)	r	$\Delta_{sol}H^{\theta}_{m}$(kJ mol^{-1})
3.23	100431	54.83
5.88	55159	54.08
8.92	36367	54.41
10.01	32400	54.30
10.47	30969	54.84
13.57	23895	54.79
15.01	21596	54.47
15.09	21489	54.74
17.33	18712	54.59
20.06	16170	54.47
21.72	14929	54.98
22.09	14679	54.25
24.36	13311	54.03
29.37	11044	54.62
	Mean	54.53±0.24

$[Dy(NTO_2(H_2O)_6]\cdot NTO\cdot 4H_2O$, and r is the molar ratio $n(H_2O)/n\{[Dy(NTO)_2(H_2O)_6]\cdot NTO\cdot 4H_2O\}$.

Because $[Dy(NTO)_2(H_2O)_6]\cdot NTO\cdot 4H_2O$ is completely ionized in aqueous solution, its ionization process can be represented as

$$[Dy(NTO)_2(H_2O)_6]\cdot NTO\cdot 4H_2O \xrightarrow{\Delta_{sol}H^\theta_m} Dy^{3+}(aq,\infty) + 3NTO^-(aq,\infty) + 10H_2O(l) \qquad (1)$$

In process (1), the greater values of r were used. Therefore, the mean of $\Delta_{sol}H^\theta_m$ in Table 5 can be considered at infinite dilution.

3.4. Standard enthalpy of formation of $[Dy(NTO)_2(H_2O)_6]\cdot NTO\cdot 4H_2O(cr)$ $\Delta_f H^\theta_m\{[Dy(NTO)_2(H_2O)_6]\cdot NTO\cdot 4H_2O, cr, 298.15\,K\}$

By substituting the mean of $\Delta_{sol}H^\theta_m$ listed in Table 5 and the reported values of $\Delta_f H^\theta_m(Dy^{3+}, aq, \infty) = -698.73\ kJ\,mol^{-1}$ [3], $\Delta_f H^\theta_m(NTO^-, aq, \infty) = -(94.3 \pm 2.1)\ kJ\,mol^{-1}$ [4], and $\Delta_f H^\theta_m(H_2O, l) = -285.83\ kJ\,mol^{-1}$ [3], into Eq. (2),

$$\begin{aligned}\Delta_f H^\theta_m\{[Dy(NTO)_2(H_2O)_6]\cdot NTO\cdot 4H_2O, cr,\\ 298.15\ K\} = \Delta_f H^\theta_m(Dy^{3+}, aq, \infty)\\ + 3\Delta_f H^\theta_m(NTO^-, aq, \infty) + 10\Delta_f H^\theta_m(H_2O, l)\\ - \Delta_{sol}H^\theta_m\}\end{aligned} \qquad (2)$$

the following value was obtained:

$$\Delta_f H^\theta_m\{[Dy(NTO)_2(H_2O)_6]\cdot NTO\cdot 4H_2O, cr, 298.15\,K\} = -(3894.5 \pm 6.5)\ kJ\,mol^{-1}.$$

3.5. Lattice enthalpy and energy of $[Dy(NTO)_2(H_2O)_6]\cdot NTO\cdot 4H_2O$

$$\Delta H^\theta_L\{[Dy(NTO)_2(H_2O)_6]\cdot NTO\cdot 4H_2O, cr\},$$
$$\Delta U^\theta_L\{[Dy(NTO)_2(H_2O)_6]\cdot NTO\cdot 4H_2O, cr\}$$

Setting $\Delta H^\theta_L\{[Dy(NTO)_2(H_2O)_6]\cdot NTO\cdot 4H_2O, cr\}$ as the lattice enthalpy in forming the crystal $[Dy(NTO)_2(H_2O)_6]\cdot NTO\cdot 4H_2O$ from $Dy^{3+}(g)$, $NTO^-(g)$ and $H_2O(g)$ at 298.15 K, and $\Delta U^\theta_L\{[Dy(NTO)_2(H_2O)_6]\cdot NTO\cdot 4H_2O, cr\}$ as the crystal lattice energy

$$Dy^{3+}(g) + 3NTO^-(g) + 10H_2O(g) \xrightarrow{\Delta H^\theta_L} [Dy(NTO)_2(H_2O)_6]\cdot NTO\cdot 4H_2O(cr) \qquad (3)$$

we have

$$\begin{aligned}\Delta H^\theta_L\{[Dy(NTO)_2(H_2O)_6]\cdot NTO\cdot 4H_2O, cr\}\\ = \Delta_f H^\theta_m\{[Dy(NTO)_2(H_2O)_6]\cdot NTO\\ \cdot 4H_2O, cr, 298.15\,K\}\\ - \Delta_f H^\theta_m(Dy^{3+}, g) - 3\Delta_f H^\theta_m(NTO^-, g)\\ - 10\Delta_f H^\theta_m(H_2O, g)\end{aligned} \qquad (4)$$

and

$$\begin{aligned}\Delta U^\theta_L\{[Dy(NTO)_2(H_2O)_6]\cdot NTO\cdot 4H_2O, cr\}\\ = \Delta H^\theta_L\{[Dy(NTO)_2(H_2O)_6]\cdot NTO\cdot 4H_2O, cr\}\\ - \Delta nRT\end{aligned} \qquad (5)$$

where $\Delta_f H^\theta_m(Dy^{3+}, g) = 4206.6\ kJ\,mol^{-1}$ [5]; $\Delta_f H^\theta_m(NTO^-, g) = -374.3\ kJ\,mol^{-1}$ [6]; $\Delta_f H^\theta_m(H_2O, g) = -241.82 kJ\,mol^{-1}$ [1]; $\Delta n = -14$; $RT = 2.5\ kJ\,mol^{-1}$.

By substituting the above-mentioned data into Eq. (4) and Eq. (5), the following values are obtained:

$$\Delta H^\theta_L\{[Dy(NTO)_2(H_2O)_6]\cdot NTO\cdot 4H_2O, cr\} = -4560\ kJ\,mol^{-1};$$
$$\Delta U^\theta_L\{[Dy(NTO)_2(H_2O)_6]\cdot NTO\cdot 4H_2O, cr\} = -4525\ kJmol^{-1}.$$

3.6. Standard enthalpy of dehydration of $[Dy(NTO)_2(H_2O)_6]\cdot NTO\cdot 4H_2O$ (cr), $\Delta H^\theta_d\{[Dy(NTO)_2(H_2O)_6]\cdot NTO\cdot 4H_2O, cr\}$

According to process (6) and Eq. (7)

$$[Dy(NTO)_2(H_2O)_6]\cdot NTO\cdot 4H_2O \xrightarrow{\Delta H^\theta_d\{[Dy(NTO)_2(H_2O)_6]\cdot NTO\cdot 4H_2O, cr\}} Dy(NTO)_3(cr) + 10H_2O(l) \qquad (6)$$

and

$$\begin{aligned}\Delta H^\theta_d\{[Dy(NTO)_2(H_2O)_6]\cdot NTO\cdot 4H_2O, cr\}\\ = \Delta_f H^\theta_m[Dy(NTO)_3, cr, 298.15\,K]\\ + 10\Delta_f H^\theta_m(H_2O, l)\\ - \Delta_f H^\theta_m\{[Dy(NTO)_2(H_2O)_6]\cdot NTO\\ \cdot 4H_2O, cr, 298.15\,K\}\end{aligned} \qquad (7)$$

the value of $\Delta H_{\mathrm{d}}^{\theta}\{[\mathrm{Dy(NTO)_2(H_2O)_6}]\cdot\mathrm{NTO}\cdot 4\mathrm{H_2O,cr}\}$ of 306.9 kJ mol^{-1} may be obtained from the value of $\Delta_{\mathrm{f}}H_{\mathrm{m}}^{\theta}\{[\mathrm{Dy(NTO)_2(H_2O)_6}]\cdot\mathrm{NTO}\}\cdot 4\mathrm{H_2O,cr,298.15\,K}\} = -3894.5\,\mathrm{kJ\,mol^{-1}}$, obtained in this work, and the reported values $\Delta_{\mathrm{f}}H_{\mathrm{m}}^{\theta}[\mathrm{Dy(NTO)_3,cr,298.15\,K}] = -729.3\,\mathrm{kJ\,mol^{-1}}$ [6], $\Delta_{\mathrm{f}}H_{\mathrm{m}}^{\theta}(\mathrm{H_2O,l}) = -285.83\,\mathrm{kJ\,mol^{-1}}$ [1].

Acknowledgements

This work is supported by the Science and Technology Foundation of the National Defence Key Laboratory of Propellant and Explosive Combustion of China.

References

[1] R.C. Weast, CRC Handbook of Chemistry and Physics, 70th edn. CRC Press Inc., Boca Raton, FL, 1989, D122.
[2] Zhang Tonglai, Hu Rongzu and Li Fuping, J. Rare Earths, 13(1) (1995) 10–15.
[3] R.C. Weast, CRC Handbook of Chemistry and Physics, 63rd edn. CRC Press Inc., Boca Raton, FL, 1982–1983, D52–95.
[4] A. Finch, P.J. Gardner, A.J. Head and H.S. Majdi, J. Chem. Thermodyn., 23(12) (1991) 1169–1173.
[5] Yi Jinzhi and Sun Tongshan, Personal Communication, 1995.
[6] Hu Rongzu, Meng Zihui and Kang Bing, Thermochim. Acta, 275 (1996) 159–172.